*Life-Cycle of Structures and Infrastructure Systems – Biondini & Frangopol (Eds)*


# The design and development of a demountable and reconfigurable segmented fan concrete shell flooring system

M. Nuh & J. Orr
*University of Cambridge, Cambridge, UK*

R. Oval
*Princeton University, Princeton, USA*

ABSTRACT: The structural floor of typical concrete frame buildings contributes a significant portion to the total embodied carbon of the superstructure by its sheer mass. In addition, the monolithic nature of in-situ concrete and the frequent use of grouting for prefabricated components result in structures which are often difficult to disassemble, creating barriers towards reuse. We present a novel segmented thin-shell concrete flooring system which facilitates component reuse and reconfiguration compatible with a circular economy for construction. By leveraging the funicular potential of shell structures and the geometry of masonry fan vaults, a lightweight materially efficient flooring system which can be disassembled without the need to cut through concrete or grout is proposed. Fabrication and assembly of a scale prototype spanning 2 m by 2 m were carried out as a proof-of-concept, leveraging digital fabrication techniques to create the curved vault profile.

## 1 INTRODUCTION

The construction industry contributes an estimated 38% of worldwide energy and process-related emissions (United Nations Environment Programme, 2020), emphasising the need for increased efforts to reduce the environmental impact of our built environment. A potential means which has gained renewed interest for reducing the carbon impact of building structures is the reuse of structural building components to extend their lifespan. However, various projects which implement concrete reuse have often faced challenges in terms of making them economical (Durmisevic, 2019; Eklund et al., 2003; Glias, 2013; Roth, 2005; te Dorsthorst & Kowalczyk, 2005); having to cut away sections manually is a labour-intensive process which typically leads to increased cost premiums, making it an economically unattractive practice.

We present a novel flooring system which is designed for disassembly, component reuse, and reconfigurability. Concrete segments can be assembled without the use of any grout through a compression-dominated segmentation plan. A geometry inspired by masonry fan vaults facilitates this segmentation while also allowing reconfiguration to span different distances. This paper will detail the design conceptualisation and form-finding approach for the shell, the potential for reconfigurability in the context of a circular economy of construction, the fabrication and assembly of a quarter-scale prototype, and, lastly, a sustainability assessment of the flooring system.

## 2 CONCEPTUAL AND STRUCTURAL DESIGN

A segmented shell flooring system offers several advantages related to carbon savings compared to conventional flat slab concrete flooring. Firstly, the funicular nature of a shell (i.e., mainly acting in compression) is highly compatible with brittle materials with low tensile capacity such as plain concrete. As such, less concrete is needed to span distances and there is no need to embed steel reinforcement within the concrete to resolve tensile stresses. Rather, the thrust of the vault can be resolved externally, either through buttresses (as is the case in Gothic cathedrals) or through external ties, creating a physical separation between the materials which

DOI: 10.1201/9781003323020-11

is conducive for disassembly and reuse. Secondly, segmentation allows for accurate prefabrication of the curved components, thereby reducing the amount of on-site concrete required. This leads to less material wastage due to the more controlled factory environment compared to on-site casting. Lastly, the compressive nature of the shell combined with the segmentation allows for dry joints under compression between segments. This facilitates disassembly as there is no need to manually cut out elements using saws or to remove grouting. As a trade-off, the complexity lies in the assembly and disassembly process of the shell which is more involved compared to the fabrication of prismatic formwork or assembly of prefabricated flat slabs.

The use of dry joints in segmented shells for flooring systems is not a novel concept: a 3D sand-printed floor using 5 discrete segments has been prototype (Rippmann et al., 2018) and a nine-segment concrete floor demonstrator spanning a 4.5 m by 4.5 m bay (Oval et al., 2023) all validates that it is a structurally feasible system. However, the primary focus of these prototypes was not on the potential for disassembly and circularity of the structure; the segmentation was typically a by-product of size constraints imposed by transportation or digital fabrication print area limitations. Reconfiguration of the structure to span different distances was also not considered as it is challenging for a form-found shell; changing the distance spanned will affect membrane action and introduce bending unless the curvature of the structure is adjusted.

To further leverage the disassembly potential of a segmented concrete shell for circularity, therefore increasing its lifespan and reducing its environmental impact, the form-finding and segmentation plan of the shell must be taken into consideration. The two are intimately interlinked to each other as the shape of the shell will affect the 'optimal' locations of interfaces. The criteria for an optimal interface were defined as follows:

1. Compression dominated to avoid opening of interfaces and hinge formation, and
2. Minimal shear forces along the surface of the interface to avoid slipping.

To satisfy both criteria, it follows that interfaces should be oriented with their normal aligned with the principal compressive stress direction.

### 2.1 *Fan vault concept*

The masonry fan vault presents a base for the shell geometry which allows for a simple segmentation plan that is both optimal and allows for reconfigurability. The geometry of the fan vault is characterised by surfaces of revolutions which form conoids which may intersect with one another, with the central region (if there are any) filled by a spandrel–a shallow or flat segment acting as a keystone. The manner in which the conoids intersect with each other defines the class of fan vault (Bagi, 2021). Here, we are mainly interested in fan vaults where the conoids do not intersect with each other, to avoid trimming segments that would become harder to reuse. The surface of revolution also allows for increased repetition of segments along the hoop direction, facilitating prefabrication and modularity.

Membrane analysis can be performed to determine a state of stresses on the conoids following plasticity's lower-bound theorem (Heyman, 1967), shown in Figure 1. Taking a strip along the conoid and applying a radially symmetric load at the top, the analysis shows that, with a sufficiently large spandrel load, the structure experiences no tensile stresses. In this radially symmetric load case, the compressive stresses flow along the strip direction with the other principal stress direction found along the hoop-wise direction of the conoids, providing an evident and simple segmentation plan. While the true loading clearly does not take the form of a constant, radially symmetric load, this provides a good starting point for the segmentation plan. In addition, the locations of interfaces having minimal shear forces will inevitably vary depending on the loading due to asymmetric load cases, making optimisation of a segmentation plan against one load case an unproductive exercise. The shear which will be present in the interfaces can be minimised by the inclusion of interlocking shear keys between segments to resist slippage. Staggering can also aid in this, although was not considered for this design as it introduces complexity to the fabrication process.

The spandrel and the conoid of the fan vault inspired shell can be separated into two parts of the system, allowing them to be uncoupled to span different distances, as shown in Figure 2. Shorter distances can be spanned by removing the sections of the upper conoids and

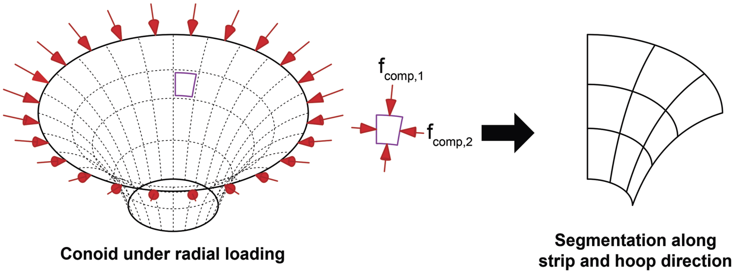


Figure 1. Conoid membrane analysis of the fan vault informing the segmentation plan for the shell.

installing a new spandrel while larger distances can be spanned by installing a larger spandrel. For the latter, the increased loading may not be sufficiently resisted by the conoids. In such cases, it may be necessary to reinforce the conoids (e.g., using carbon fibre plates or wraps) unless the shell was already pre-designed for a larger span. Note that if a different distance is to be spanned, this requires the fabrication of a new spandrel, leading to waste. However, the flexibility the system affords for future reuse cases may prove beneficial; while it has been suggested that a *form follows availability* approach should be taken for a design using reused components (Brütting et al., 2019), increased flexibility in the distance spanned allows designers more freedom in the final form and may lower the barrier towards reuse.

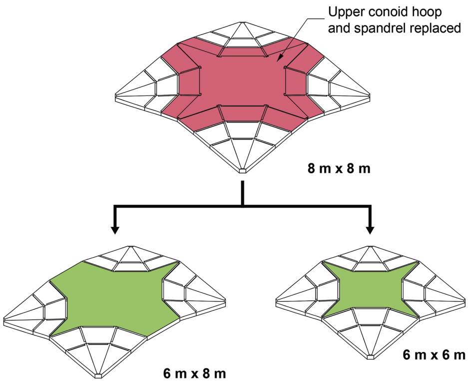


Figure 2. Reuse of a segmented fan concrete shell to span different bay sizes.

### 2.2 *Form finding and structural optimisation*

Form finding of the segmented fan concrete shell was performed by firstly parametrising the geometry into the thicknesses at various locations and the curve profile of the conoid, illustrated in Figure 3. This was performed in the Grasshopper visual programming environment (Rutten et al., 2007). The shape of the curve was controlled by a Bézier curve with 4 control points, with the two endpoints set by the shell width and depth. The coordinates for the Bézier curve's profile were limited to the upper triangle to ensure a concave profile. The thickness in the conoid was allowed to vary linearly (against the u-direction shown in Figure 3) from the base to the top and a separate constant thickness was allowed for the spandrel. The span of this shell was set as a constant 8 m and the distance from the mid-depth of the spandrel to the mid-depth of the conoid base was set to 800 mm. This was selected as a representative span and depth, although different spans can be easily optimised for using the same approach. Segmentation along the strip direction was done every 1 m as this is assumed to provide a sufficiently small resolution for reconfiguration purposes while avoiding too many segmentations which results in a lower structural capacity. As it is envisioned that the smallest distance between columns will be at least 4 m, the segments in a 2 m vicinity from each corner were merged. M24 steel ties were connected at the corners to resolve the horizontal thrust of the shell.

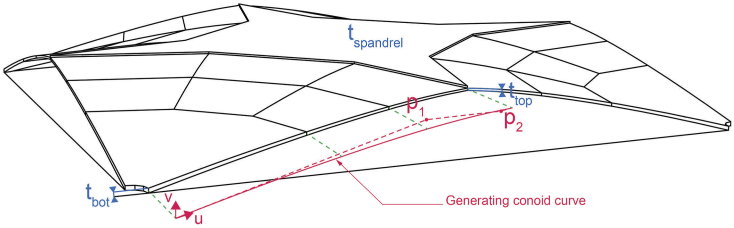


Figure 3. Parametrized geometry model.

Using the shell geometry parametrised into 7 variables (with the two points deconstructed into their coordinate values), a finite element model in Karamba3D (Preisinger & Heimrath, 2014) was created using shell elements to ensure that the element stresses are within the material limits and that the shell is stable. In addition to the gravitational loading, a uniform imposed load of 1 kPa and a live load of 1.5 kPa were applied. The lower live load was selected based on work by Orr (2018) which suggested it is a more representative loading for a typical office building. Various area loading was applied to the shell and preliminary investigations show that the uniform live load case was likely to be critical. As such, optimisation was carried out based on that load case.

A unique modelling approach for the interfaces was taken, inspired by one developed for a rigid body analysis (Galassi et al., 2018). At the interface, stiff beam elements are connected to nodes located at the extreme fibre locations. The beams are removed if tensile forces are transmitted across the nodes, allowing 1) a hinge to form at the interface and 2) the segments to fully detach themselves. The beam elements are added back in if the nodes are detected to penetrate each other, signifying a closing of the interface. The use of a stiff beam element is due to the lack of rigid links in Karamba3D. Analysis was performed by incrementally increasing the loading by 10% for a linear elastic model where the interface elements were modified for each iteration. Note that this is not a non-linear analysis, but rather a set of linear elastic analyses where the previous analysis informs the state of the joints of the next. As such, it will not fully capture the behaviour of the structure, especially in cases where many hinges form as the model will exhibit large rotations and displacements. A fully non-linear analysis incorporating contact behaviour using commercial software such as 3DEC and LS-DYNA is expected to be able to capture the behaviour of the shell. However, the long computation time is not conducive for optimisation purposes, often taking several days to compute a single shell.

The Wallacei Grasshopper plugin (Makki et al., 2021), which implements the NSGA-II multi-objective evolutionary algorithm (Deb et al., 2002) was used to optimise the shell against two objectives: maximised buckling load factor and minimised mass (which was used as a surrogate metric for the embodied carbon of the structure). Once the algorithm converged, a set of Pareto front solutions was obtained which provides a minimum mass structure given a certain buckling load factor. Due to the limitations of the linear elastic analysis used, as well as to account for manufacturing tolerances, a candidate with a large buckling load factor of 10 (the properties of which are tabulated in Table 1) was selected for the basis of design for the fabricated quarter-scale prototype spanning 2 m by 2 m. As the thicknesses of the quarter-scale prototype were quite thin (being merely 18 mm at the top of the conoid), all the thicknesses were doubled to accommodate fabrication process tolerances and prevent significant damage from storage and handling.

## 3 FABRICATION

Fabrication of variable-thickness curved concrete shells poses challenges on two fronts: the manufacturing of the formwork and the deposition of the material. The Automated Robotic Concrete Spraying fabrication process (Nuh et al., 2022) was developed to address these challenges and was used to fabricate the curved conoid segments (Figure 4). Using a target spraying surface constructed using a wooden frame and a shape-reconfigurable pin-bed, a robot arm connected to a glass fibre reinforced concrete (GFRC) spraying station deposits the

Table 1. Selected candidate from form finding optimisation.

| | Selected candidate's properties |
|---|---|
| *Objective values* | |
| Mass | 10.8 t |
| Buckling load factor | 10.2 |
| *ULS stress and utilisation* | |
| Steel tie | 489 MPa (67.7%) |
| GFRC tensile | 3.34 MPa (87.3%) |
| GFRC compressive | 4.93 MPa (23.7%) |
| *Variables [full-scale geometry]* | |
| Conoid thickness – bottom [$t_{bot}$] | 100 mm |
| Conoid thickness – top [$t_{top}$] | 75 mm |
| Spandrel thickness [$t_{spandrel}$] | 86 mm |
| Bézier point 1 [$p_1$] | (1.94, 0.43) m |
| Bézier point 2 [$p_2$] | (3.48, 0.70) m |

material where it is required. The shear keys were formed by including their negatives within the wooden frame. As the spandrel was of a flat profile, it was not manufactured using this process and was instead cast in a conventional manner using wooden formwork. Further details regarding the GFRC mix can be found in Nuh et al. (2022) and the unreinforced spandrel was cast using a standard C30/37 class concrete mix.


Figure 4. Digital fabrication setup (left) used to fabricate the sprayed GFRC conoid segments (right).

## 4 ASSEMBLY AND DISASSEMBLY

The assembly of the segmented fan concrete shell requires that all pieces are placed in their correct position before being decentred. As opposed to masonry structures which often require intricate falsework and scaffolding due to the large number of bricks, the shell's larger segments mean that telescopic props and standard scaffolding can be used to position the structure as needed. The addition of shear keys also aids in the erection process as they align adjacent segments together. A similar method was used to great effect by Oval et al. (2023) to assemble their nine-segment shell demonstrator.

The detailed procedure for the assembly of the prototype shell is as follows, also illustrated in Figure 5:

1. Position all segments in their appropriate location using props and jacks,
2. Tighten the steel ties to resolve the horizontal thrust from the shell's self-weight, and
3. Remove the props.

For the prototype, the fabrication tolerances of the hand-made wooden side frames were found to be lacking. This resulted in gaps between segments, which ranged from effectively flush to 1 cm (i.e., approximately 2% of their size), hindering solid contact and arch action formation. Therefore, fine sand was added between the interfaces prior to tightening the steel ties. This was found to sufficiently stabilise the shell while still being demountable. The fully assembled shell is shown in Figure 6.

The disassembly process of the shell follows the same procedure as the assembly process but in reverse; by adding props and slightly pushing on the segments, the tie can be safely loosened, and the segments lifted off one by one.

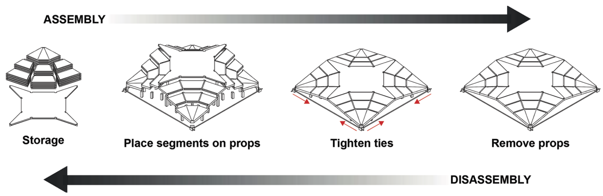


Figure 5. Assembly and disassembly process for the shell.

Figure 6. The prototype segmented fan concrete shell during assembly (left) and fully assembled (right).

## 5 SUSTAINABILITY ASSESSMENT

The embodied carbon impacts from *cradle-to-gate* (Modules A1 to A3 of the BS EN 15798 life cycle stages) of various flooring systems were compared to provide a quantitative comparison of their carbon impact. The selected flooring systems compared are:

1. Flat concrete slab,
2. BubbleDeck (a voided hollow deck system), and
3. Segmented fan concrete shell.

Combined embodied carbon factors for the relevant materials are tabulated in Table 2. For this analysis, the flat concrete slab, BubbleDeck, and the flat spandrel of the segmented shell were designed using C30/37 class concrete with 35% cement replacement and reinforcement bars having a yield stress of 500 MPa. The design was based on an 8 m by 8 m bay under the same loading as the segmented shell based on Eurocode 2 for the flat slab and recommendations from the BubbleDeck manufacturer for the voided hollow deck system (BubbleDeck, 2006). The HDPE bubble thickness used to form the BubbleDeck voids was assumed to be 5 mm. Excluded from the calculation is the raised flooring–which will be used to create a level surface for the shell like the demonstrator shell by Oval et al. (2023)–as it is assumed that all flooring systems will include them to accommodate services. The resulting masses and the embodied carbon equivalents of the three flooring systems are tabulated in Table 3.

The analysis shows that the segmented fan concrete shell has a lower embodied carbon impact compared to the other options, albeit only a 13.6% saving compared to the reference flat slab. This is mainly due to the high embodied carbon of the GFRC mix which has a high proportion of cement. This saving can be further increased by using larger aggregates and by adding cement replacement as binder. Conversely, the 8 m by 8 m span used to design the flat slab and BubbleDeck are not optimal spans for those systems; shorter spans have been shown to reduce the initial embodied carbon contribution of these reinforced concrete systems (Drewniok, 2020) making them potentially competitive with the segmented fan concrete shell. However, one clear benefit of

Table 2. Cradle-to-gate embodied carbon factors of materials.

| Material | Embodied carbon factor kgCO2e/kg |
|---|---|
| C30/37 with 35% cement replacement[1] | 0.103 |
| Reinforcement bars/steel ties[2] | 0.76 |
| HDPE[3] | 1.93 |
| Plywood formwork[4] | 0.681 |
| *GFRC components* | |
| Cement[4] | 0.832 |
| Sand[4] | 0.00747 |
| Polycure FT [curing agent][4,5] | 1.67 |
| Flowaid FT [super plasticizer][4] | 1.88 |
| Pumpaid FT [thixotropic pumping aid][4,5] | 1.67 |
| Alkali resistant glass fibre[6] | 3.00 |
| Combined GFRC mix | 0.626 |

1 (Institut Bauen und Umwelt e.V, 2018)
2 (UK CARES, 2020), steel ties assumed to have similar values to reinforcement bars
3 (Hammond & Jones, 2011)
4 (Hammond & Jones, 2020)
5 Taken from average factor of concrete admixtures
6 (Granta Design Ltd, 2018)

Table 3. Mass and embodied carbon equivalent per floor area of various flooring systems.

| | Mass and embodied carbon equivalent Kg/m$^2$ and kgCO2e/m$^2$ | | | | | |
|---|---|---|---|---|---|---|
| | *Flat slab* | | *BubbleDeck* | | *Segmented fanconcrete shell* | |
| Concrete | 587.5 | 60.5 | 431.2 | 44.4 | 49.5 | 5.10 |
| Reinforcement bars/ steel ties | 40.8 | 31.0 | 38.6 | 29.4 | 1.50 | 1.14 |
| HDPE | - | - | 12.28 | 23.7 | - | - |
| GFRC | - | - | - | - | 128.1 | 80.2 |
| Plywood formwork* | 12.96 | 8.83 | 12.96 | 8.83 | 0.416 | 0.283 |
| Total | 628 (ref.) | 100.3 (ref.) | 482 (-23%) | 106.3 (+6%) | 179.1 (-71%) | 86.7 (-13%) |

* Based on a nominal weight of 720 kg/m$^3$ using 18 mm plywood.

the shell is the large mass savings of 71% over the baseline flat slab. This can result in drastic savings in the material of the columns and footings of the structure, leading to further carbon savings elsewhere in the structure. In addition, the potential for reconfiguration and design for reuse for different spans remains a strong benefit of the shell system for sustainability reasons.

## 6 CONCLUSIONS

The segmented fan concrete shell presented is a novel concrete flooring system which is designed for reuse in a circular economy. Using the revolution geometry of the fan vault provides a simple segmentation plan which facilitates reconfiguration into different spans. The quarter-scale prototype demonstrates that the system is structurally sound and can be assembled and disassembled using simple props.

To validate the modelling approach as well as investigate the structural capacity and reconfigurability of the system, an experimental testing program is currently underway. Further work is required to reduce the tolerance of the segments to provide better contact at interfaces for future prototypes. Lastly, further improvements to the mix design of the GFRC material can lead to further reductions to the cradle-to-gate embodied carbon of the structure.

## REFERENCES


Bagi, K. (2021). Statics of fan vaulting: Current state of knowledge and open issues. *Proceedings of the Royal Society A: Mathematical, Physical and Engineering Sciences*, *477*(2246), 20200893. https://doi.org/10.1098/rspa.2020.0893.

Brütting, J., Senatore, G., & Fivet, C. (2019). Form Follows Availability – Designing Structures Through Reuse. *Journal of the International Association for Shell and Spatial Structures*, *60*(4), 257–265. https://doi.org/10.20898/j.iass.2019.202.033.

BubbleDeck. (2006). *BubbleDeck Span Guide*. BubbleDeck.

Deb, K., Pratap, A., Agarwal, S., & Meyarivan, T. (2002). A fast and elitist multiobjective genetic algorithm: NSGA-II. *IEEE Transactions on Evolutionary Computation*, *6*(2), 182–197. https://doi.org/10.1109/4235.996017.

Drewniok, M. P. (2020). *Relationships between building structural parameters and embodied carbon. Part 1: Early-stage design decisions* (ENG-TR.013). University of Cambridge.

Durmisevic, E. (2019). *The Super Circular Estate project Journal N° 3*. Urban Innovative Actions.

Eklund, M., Dahlgren, S., Dagersten, A., & Sundbaum, G. (2003). *The Conditions and Constraints for Using Reused Materials in Building* Projects. 287.

Galassi, S., Misseri, G., Rovero, L., & Tempesta, G. (2018). Failure modes prediction of masonry voussoir arches on moving supports. *Engineering Structures*, *173*, 706–717. https://doi.org/10.1016/j.engstruct.2018.07.015.

Glias, A. (2013). *The 'Donor Skelet': Designing with reused structural concrete elements* [MSc]. TU Delft.

Granta Design Ltd. (2018). *The Cambridge Engineering Selector EduPack 2018* (18.1.1). Granta Design. www.grantadesign.com/industry/products/ces-selector/

Hammond, G., & Jones, C. (2011). *Embodied Carbon—The ICE Database*.

Hammond, G., & Jones, C. (2020). *Embodied Carbon—The ICE Database*.

Heyman, J. (1967). Spires and fan vaults. *International Journal of Solids and Structures*, *3*(2), 243–257. https://doi.org/10.1016/0020-7683(67)90073-X.

Institut Bauen und Umwelt e.V. (2018). *Environmental Product Declaration: UK manufactured generic ready-mixed concrete*.

Makki, M., Showkatbakhsh, M., & Song, Y. (2021). *Wallacei: An evolutionary and Analytic Engine for Grasshopper 3D* (2.65). https://www.wallacei.com/

Nuh, M., Oval, R., Orr, J., & Shepherd, P. (2022). Digital fabrication of ribbed concrete shells using automated robotic concrete spraying. *Additive Manufacturing*, *59*, 103159. https://doi.org/10.1016/j.addma.2022.103159.

Orr, J. (2018). *Minimising Energy in Construction*. University of Cambridge.

Oval, R., Nuh, M., Costa, E., Madyan, O. A., Orr, J., & Shepherd, P. (2023). A prototype low-carbon segmented concrete shell building floor system. *Structures*, *49*, 124–138. https://doi.org/10.1016/j.istruc.2023.01.063.

Preisinger, C., & Heimrath, M. (2014). Karamba—A Toolkit for Parametric Structural Design. *Structural Engineering International*, *24*(2), 217–221. https://doi.org/10.2749/101686614X13830790993483

Rippmann, M., Liew, A., Van Mele, T., & Block, P. (2018). Design, fabrication and testing of discrete 3D sand-printed floor prototypes. *Materials Today Communications*, *15*, 254–259. https://doi.org/10.1016/j.mtcomm.2018.03.005

Roth, L. (2005). *Reuse of construction materials—Environmental performance and assessment methodology* [PhD]. Linköpings universitet.

Rutten, D., McNeel, R., & others. (2007). *Grasshopper3D*. Robert McNeel & Associates.

te Dorsthorst, B. J. H., & Kowalczyk, T. (2005). State of Deconstruction in the Netherlands. In *Deconstruction and Materials Reuse—An International Overview* (Vol. 300). in - house publishing.

UK CARES. (2020). *Environmental Product Declaration: Carbon Steel Reinforcing Bar (secondary production route—Scrap), Sector Average*.

United Nations Environment Programme. (2020). *2020 Global Status Report for Buildings and Construction: Towards a Zero-emission, Efficient and Resilient Buildings and Construction Sector*. United Nations Environment Programme.